

Transverse Mercator with an accuracy of a few nanometers

Charles F. F. Karney*

SRI International, 201 Washington Rd, Princeton, NJ 08543-5300

(Dated: February 8, 2010; revised February 3, 2011)

Implementations of two algorithms for the transverse Mercator projection are described; these achieve accuracies close to machine precision. One is based on the exact equations of Thompson and Lee and the other uses an extension of Krüger's series for the mapping to higher order. The exact method provides an accuracy of 9 nm over the entire ellipsoid, while the errors in the series method are less than 5 nm within 3900 km of the central meridian. In each case, the meridian convergence and scale are also computed with similar accuracy. The speed of the series method is competitive with other less accurate algorithms and the exact method is about 5 times slower.

Keywords: geometrical geodesy, map projections, conformal mapping

1. INTRODUCTION

The transverse Mercator or Gauss–Krüger projection is a conformal mapping of the earth ellipsoid where a central meridian is mapped into a straight line at constant scale. Because it cannot be expressed in terms of elementary functions, the mapping is usually computed by means of a truncated series (Krüger, 1912; Thomas, 1952). The resulting mapping approximates the true mapping only within a region centered on the central meridian.

Transverse Mercator is one of the commonest projections used for large-scale maps (it is used for the grid systems of several countries and is the basis of the universal transverse Mercator (UTM) system (Hager *et al.*, 1989, Chap. 2)). For the WGS84 ellipsoid, the variation of the scale is 1.25% within 1000 km of the central meridian; it is therefore desirable to find algorithms for the mapping which are accurate to machine precision over at least this area. In this paper, I describe the implementation of two such algorithms, one based on the exact equations given by Lee (1976) and the other extending the series given by Krüger (1912) to higher order. Both implementations compute the forward and reverse mappings and also return the meridian convergence and scale. These implementations are included in GeographicLib (Karney, 2010).

Scores of other authors have presented methods for computing this mapping over the past century. In particular, Dozier (1980) provided an implementation of Lee's exact method, and Engsager and Pöder (2007) give Krüger's series to 7th order. The distinguishing aspects of this work are the reduction of the overall numerical errors (truncation and round-off) to close to the precision limit of the computer and the concrete bounds I place on these errors.

Because floating-point numbers have a finite spacing (Olver *et al.*, 2010, §3.1(i)), the limiting accuracy of any implementation is about $M/2^p$ where $M = 10\,000$ km is the length of the quarter meridian of the earth and p is the number of bits in the fraction of the floating-point number system. This gives an error limit of 0.5 m for $p = 24$ (single precision or float), 1 nm for $p = 53$ (double precision or double), and 0.5 pm for $p = 64$ (extended precision or long double). (Here, I use SI prefixes: 1 nm = 10^{-9} m, 1 pm = 10^{-12} m.) Typically $p = 24$ is too inaccurate to be useful and I don't consider this further in this paper. My standard working precision is double and the resulting accuracy, if it can be achieved, would satisfy most needs. However, I also use extended precision as one of the tools to verify the accuracy of the double precision implementations.

Formulas for mappings can contain expressions which are numerically ill-conditioned causing precision to be lost. This loss of precision is of little consequence if the truncation errors are of the same order. However, in attempting to minimize the numerical errors, I needed an accurate means of quantifying the truncation and round-off errors. To this end, I constructed a large test set of projected points which were computed with an accuracy of 80 decimal digits. This allowed me to eliminate many sources of round-off error. The resulting accuracies are about 4–8 times the limiting value (equivalent to a loss of only 2–3 bits of precision) and this applies to both double and extended precisions.

In Sect. 2, I review the series method given by Krüger (1912) modifying it to minimize the round-off errors. I turn next, Sect. 3, to the formulation of the exact transverse Mercator projection by Lee (1976) which I use to construct the high-precision test set; I also describe its implementation using double precision and I quantify the round-off errors. I extend Krüger's series to 8th order (see Sect. 4) and give the truncation error for the series as a function of truncation level and distance from the central meridian. Finally, in Sect. 5, I discuss some of the properties of the exact mapping far from

*Electronic address: charles.karney@sri.com

the central meridian.

2. KRÜGER'S SERIES

I summarize here the method developed by Krüger (1912, §§5–8), simplifying it and adapting it for optimal implementation on a computer. The method is also briefly described by Bugayevskiy and Snyder (1995, §5.1.6). The method entails mapping the ellipsoid to the conformal sphere and for this reason I begin by describing the spherical transverse Mercator projection.

Consider a sphere and a point on that sphere of latitude ϕ' and longitude relative to the central meridian of λ . (I use primes on variables, e.g., ϕ' , where necessary, to distinguish them from their ellipsoidal counterparts.) The isometric latitude is given by

$$\psi' = \text{gd}^{-1} \phi', \quad (1)$$

where

$$\text{gd} x = \int_0^x \text{sech} t dt = \tan^{-1} \sinh x = \sin^{-1} \tanh x$$

is the Gudermannian function given by Olver *et al.* (2010, §4.23(viii)) (henceforth referred to as DLMF, the Digital Library of Mathematical Functions) and

$$\text{gd}^{-1} x = \int_0^x \sec t dt = \sinh^{-1} \tan x = \tanh^{-1} \sin x$$

is its inverse. The standard (equatorial) Mercator projection maps the sphere onto the plane (λ, ψ') . When working with conformal mappings it is often useful to represent coordinates with complex numbers where the real part represents the northing and the imaginary part the easting (the phase, or argument, of the complex number gives a bearing measured *clockwise*). In this representation the Mercator projection (a conformal mapping) is given by

$$\chi = \psi' + i\lambda.$$

Any analytic function of χ also represents a conformal mapping (except where its derivative vanishes); its derivative gives the change in the meridian convergence and scale for the mapping. In particular (Lee, 1976, Eq. (12.3)),

$$\zeta' = \text{gd} \chi = \text{gd}(\psi' + i\lambda) \quad (2)$$

gives the transverse Mercator projection of the sphere. This is easy to confirm by evaluating the mapping for $\lambda = 0$; this gives $\zeta' = \phi'$, i.e., the central meridian is mapped to a straight line at constant scale (the defining property of the mapping).

I consider now an ellipsoid of revolution with equatorial radius a , polar semi-axis b , flattening $f = (a - b)/a$, eccentricity $e = \sqrt{f(2 - f)}$, and third flattening $n = (a - b)/(a + b) = f/(2 - f)$. For a point with latitude ϕ and longitude λ , the isometric latitude is given by (Lambert, 1772, §117)

$$\psi = \log \tan \left(\frac{\pi}{4} + \frac{\phi}{2} \right) - \frac{1}{2} e \log \left(\frac{1 + e \sin \phi}{1 - e \sin \phi} \right),$$

Using the identities DLMF, Eqs. (4.23.42) and (4.37.24), this relation may also be written as

$$\psi = \text{gd}^{-1} \phi - e \tanh^{-1}(e \sin \phi). \quad (3)$$

As in the case of the sphere, $\chi = \psi + i\lambda$ defines the Mercator projection. Equating the isometric latitude for the sphere with that for the ellipsoid, $\psi' = \psi$, defines a relation

$$\phi' = \text{gd}(\text{gd}^{-1} \phi - e \tanh^{-1}(e \sin \phi)), \quad (4)$$

which maps a point on the ellipsoid with latitude ϕ conformally to a point on the sphere with latitude ϕ' . In this context, ϕ' is called the “conformal latitude” and the sphere is referred to as the “conformal sphere.” The transformation to ζ' , Eq. (2), where ψ is given by Eq. (3), defines a conformal mapping of the ellipsoid to a plane in which the central meridian is mapped to a straight line with a scale which is nearly constant (the variation is $O(f)$). I call this the “spherical transverse Mercator projection” as it is the simplest generalization of the spherical projection to the ellipsoid. The graticule for this mapping is shown in Fig. 1(a). Krüger (1912, §8) now “rectifies” this mapping by applying a near-identity transformation to ζ' to make the scale constant which yields the Gauss–Krüger mapping $\zeta = \xi + i\eta$ with

$$\zeta = \zeta' + \sum_{j=1}^{\infty} \alpha_j \sin 2j\zeta', \quad (5)$$

where α_j is real (this form for the transformation is derived in Sect. 4). Similarly the transformation from ζ' to ζ can be written as

$$\zeta' = \zeta - \sum_{j=1}^{\infty} \beta_j \sin 2j\zeta, \quad (6)$$

where β_j is real. Krüger’s expressions for α_j and β_j are given below, Eqs. (12) and (17), and we outline their derivation in Sect. 4.

First, I address the computation of ζ' given ϕ and λ with special emphasis on maintaining numerical accuracy. Following Krüger, I write $\zeta' = \xi' + i\eta'$ and give separate equations for ξ' and η' . However, in order to maintain accuracy near $\phi = \pm \frac{1}{2}\pi$, I use $\tau = \tan \phi$ and $\tau' = \tan \phi'$ and eliminate ϕ' and ψ' from the relations. An expression for τ' is found by taking the tangent of Eq. (4) and using the addition rule for the hyperbolic sine to give

$$\tau' = \tau \sqrt{1 + \sigma^2} - \sigma \sqrt{1 + \tau^2}, \quad (7)$$

where

$$\tau = \tan \phi, \quad (8)$$

$$\sigma = \sinh(e \tanh^{-1}(e\tau/\sqrt{1 + \tau^2})). \quad (9)$$

Eliminating ϕ' from the expressions for ξ' and η' (Krüger, 1912, Eq. (8.36)) yields

$$\begin{aligned} \xi' &= \tan^{-1}(\tau'/\cos \lambda), \\ \eta' &= \sinh^{-1}(\sin \lambda / \sqrt{\tau'^2 + \cos^2 \lambda}). \end{aligned} \quad (10)$$

Splitting Eq. (5) into real and imaginary parts gives

$$\begin{aligned}\xi &= \xi' + \sum_{j=1}^{\infty} \alpha_j \sin 2j\xi' \cosh 2j\eta', \\ \eta &= \eta' + \sum_{j=1}^{\infty} \alpha_j \cos 2j\xi' \sinh 2j\eta',\end{aligned}\quad (11)$$

where (Krüger, 1912, Eq. (8.41))

$$\begin{aligned}\alpha_1 &= \frac{1}{2}n - \frac{2}{3}n^2 + \frac{5}{16}n^3 + \frac{41}{180}n^4 + \dots, \\ \alpha_2 &= \frac{13}{48}n^2 - \frac{3}{5}n^3 + \frac{557}{1440}n^4 + \dots, \\ \alpha_3 &= \frac{61}{240}n^3 - \frac{103}{140}n^4 + \dots, \\ \alpha_4 &= \frac{49561}{161280}n^4 + \dots.\end{aligned}\quad (12)$$

Finally, ξ and η are scaled to give the transverse Mercator easting x and northing y ,

$$x = k_0 A \eta, \quad y = k_0 A \xi, \quad (13)$$

where k_0 is the scale on the central meridian, $2\pi A$ is the circumference of a meridian, and (Krüger, 1912, Eq. (5.5))

$$A = \frac{a}{1+n} \left(1 + \frac{1}{4}n^2 + \frac{1}{64}n^4 + \dots \right). \quad (14)$$

Typically k_0 is chosen to be slightly less than 1 to minimize the deviation of the scale from unity in some region around the central meridian.

Converting from transverse Mercator to geographic coordinates entails reversing these steps. Equations (13) give

$$\eta = x/(k_0 A), \quad \xi = y/(k_0 A). \quad (15)$$

Krüger (1912, §7) writes ζ' in terms of ζ by inverting Eq. (11) to give

$$\begin{aligned}\xi' &= \xi - \sum_{j=1}^{\infty} \beta_j \sin 2j\xi \cosh 2j\eta, \\ \eta' &= \eta - \sum_{j=1}^{\infty} \beta_j \cos 2j\xi \sinh 2j\eta,\end{aligned}\quad (16)$$

where (Krüger, 1912, Eq. (7.26*))

$$\begin{aligned}\beta_1 &= \frac{1}{2}n - \frac{2}{3}n^2 + \frac{37}{96}n^3 - \frac{1}{360}n^4 + \dots, \\ \beta_2 &= \frac{1}{48}n^2 + \frac{1}{15}n^3 - \frac{437}{1440}n^4 + \dots, \\ \beta_3 &= \frac{17}{480}n^3 - \frac{37}{840}n^4 + \dots, \\ \beta_4 &= \frac{4397}{161280}n^4 + \dots.\end{aligned}\quad (17)$$

Inverting Eq. (10) gives (Krüger, 1912, Eq. (7.25))

$$\begin{aligned}\tau' &= \sin \xi' / \sqrt{\sinh^2 \eta' + \cos^2 \xi'}, \\ \lambda &= \tan^{-1}(\sinh \eta' / \cos \xi').\end{aligned}\quad (18)$$

Equation (7) may be inverted by Newton's method,

$$\tau_i = \begin{cases} \tau', & \text{for } i = 0, \\ \tau_{i-1} + \delta\tau_{i-1}, & \text{otherwise,} \end{cases} \quad (19)$$

$$\tau'_i = \tau_i \sqrt{1 + \sigma_i^2} - \sigma_i \sqrt{1 + \tau_i^2}, \quad (20)$$

$$\delta\tau_i = \frac{\tau' - \tau'_i}{\sqrt{1 + \tau_i'^2}} \frac{1 + (1 - e^2)\tau_i'^2}{(1 - e^2)\sqrt{1 + \tau_i'^2}}. \quad (21)$$

This usually converges to round-off after two iterations, i.e., $\tau = \tau_2$, which gives

$$\phi = \tan^{-1} \tau. \quad (22)$$

The meridian convergence and scale can be found during the forward mapping by differentiating Eq. (5) and writing

$$p' - iq' = \frac{d\zeta}{d\zeta'},$$

or

$$p' = 1 + \sum_{j=1}^{\infty} 2j\alpha_j \cos 2j\xi' \cosh 2j\eta', \quad (23)$$

$$q' = \sum_{j=1}^{\infty} 2j\alpha_j \sin 2j\xi' \sinh 2j\eta'.$$

Then the meridian convergence (the bearing of grid north, the y axis, measured clockwise from true north) is given by $\gamma = \gamma' + \gamma''$, where (Krüger, 1912, Eqs. (8.44–45))

$$\begin{aligned}\gamma' &= \tan^{-1}((\tau'/\sqrt{1 + \tau'^2}) \tan \lambda), \\ \gamma'' &= \tan^{-1}(q'/p').\end{aligned}\quad (24)$$

The scale is given by $k = k_0 k' k''$, where (Krüger, 1912, Eq. (8.47))

$$\begin{aligned}k' &= \sqrt{1 - e^2 \sin^2 \phi} \sqrt{1 + \tau^2} / \sqrt{\tau'^2 + \cos^2 \lambda}, \\ k'' &= \frac{A}{a} \sqrt{p'^2 + q'^2}.\end{aligned}\quad (25)$$

Here γ' and k' give the convergence and scale for the spherical transverse Mercator projection, while γ'' and k'' give the corrections due to Eqs. (5) and (13).

To determine the convergence and scale during the reverse mapping, differentiate Eq. (6) and write

$$p + iq = \frac{d\zeta'}{d\zeta} = \frac{1}{p' - iq'},$$

or

$$p = 1 - \sum_{j=1}^{\infty} 2j\beta_j \cos 2j\xi \cosh 2j\eta, \quad (26)$$

$$q = \sum_{j=1}^{\infty} 2j\beta_j \sin 2j\xi \sinh 2j\eta.$$

The convergence is given by $\gamma = \gamma' + \gamma''$, where (Krüger, 1912, Eqs. (7.31–31*))

$$\begin{aligned}\gamma' &= \tan^{-1}(\tan \xi' \tanh \eta'), \\ \gamma'' &= \tan^{-1}(q/p).\end{aligned}\quad (27)$$

The scale is given by $k = k_0 k' k''$, where (Krüger, 1912, Eq. (7.33))

$$\begin{aligned}k' &= \sqrt{1 - e^2 \sin^2 \phi} \sqrt{1 + \tau^2} \sqrt{\sinh^2 \eta' + \cos^2 \xi'}, \\ k'' &= \frac{A}{a} \frac{1}{\sqrt{p^2 + q^2}}.\end{aligned}\quad (28)$$

In summary, Krüger's methods for the forward and reverse mappings are given by the numbered Eqs. (7)–(14) and Eqs. (14)–(22), respectively. The scale and meridian convergence are similarly given by the Eqs. (23)–(25) during the forward mapping and Eqs. (26)–(28) during the reverse mapping.

Krüger truncates the series at order n^4 , as shown here. This results in very small errors, considering that Krüger published his paper in 1912. The maximum of the errors for the forward and reverse mappings (both expressed as true distances) is $0.31 \mu\text{m}$ within 1000 km of the central meridian and is 1 mm within 6000 km of the central meridian. The truncated mapping is exactly conformal; however Eqs. (5) and (6) are not inverses of one another if the sums are truncated. It is, of course, possible to construct an exact inverse of the truncation of Eq. (5), e.g., by solving it using Newton's method. However, in practice, it is better merely to retain enough terms in the sum so that the truncation error is less than the round-off error.

In numerically implementing this method, the terms A , α_j , and β_j , Eqs. (14), (12), and (17), need only be computed once for a given ellipsoid and, for accuracy and speed, should be evaluated in Horner form (DLMF, §1.11(i)); for example, α_1 is evaluated to order n^4 as

$$\alpha_1 = \left(\frac{1}{2} + \left(-\frac{2}{3} + \left(\frac{5}{16} + \frac{41}{180}n\right)n\right)n\right)n.$$

Furthermore the trigonometric series, Eqs. (11), (16), (23), and (26), can be evaluated using Clenshaw (1955) summation (DLMF, §3.11(ii)) which minimizes the number of evaluations of trigonometric and hyperbolic functions. Thus Eqs. (11) and (23) may be summed to order J with

$$\begin{aligned}c_{J+1} &= c_{J+2} = 0, \\ c_j &= 2c_{j+1} \cos 2(\xi' + i\eta') - c_{j+2} + \alpha_j, \\ \xi + i\eta &= \xi' + i\eta' + c_1 \sin 2(\xi' + i\eta'),\end{aligned}$$

and

$$\begin{aligned}d_{J+1} &= d_{J+2} = 0, \\ d_j &= 2d_{j+1} \cos 2(\xi' + i\eta') - d_{j+2} + 2j\alpha_j, \\ p' + iq' &= 1 - d_2 + d_1 \cos 2(\xi' + i\eta'),\end{aligned}$$

separated into real and imaginary parts and with the recursion relations for c_j and d_j evaluated for $J \geq j > 0$. The summations of Eqs. (16) and (26) are handled in a similar fashion.

My introduction to Krüger's expansion was a report by the Finnish Geodetic Institute (Kuittinen *et al.*, 2006). The method described here follows this report with a few changes to improve the numerical accuracy: (a) I use more stable formulas for converting from geographic to the spherical transverse Mercator coordinates; (b) I solve for the geographic latitude by Newton's method instead of by iteration; and (c) I use Krüger's method for determining the convergence and scale instead of less accurate expansions in the longitude.

In contrast to the series given here, the formulas given by Krüger in a later section of his paper, §14, involve an expansion in the longitude difference instead of the flattening. This expansion forms the basis of the approximate transverse Mercator formulas presented by Thomas (1952, pp. 2–6) and in the report on UTM (Hager *et al.*, 1989, Chap. 2) and are used in Geotrans (2010). For computing UTM coordinates, the errors are less than 1 mm. Unfortunately, the truncated series does not define an exact conformal mapping. In addition, in some applications, use of these series may lead to unacceptably large errors. For example, consider mapping Greenland with transverse Mercator with a central meridian of 42° W. The landmass of Greenland lies within 750 km of this central meridian and the maximum variation in the scale of transverse Mercator is only 0.7%—in other words, the transverse Mercator projection is ideal for this application. The error in computing transverse Mercator with Krüger's 4th order series is (as we have seen) less than $1 \mu\text{m}$. However the maximum error using Thomas' series (as implemented in Geotrans, version 3.0) is over 1 km.

3. EXACT MAPPING

The definition of the transverse Mercator projection given at the beginning of Sect. 1 serves to specify the mapping completely. (There are two minor qualifications to this statement: the central scale, the origin, and the orientation of the central meridian need to be specified; in addition, the mapping becomes multi-valued very far from the central meridian as detailed in Sect. 5.) Provided that the series in Eqs. (5), (6), and (14) are convergent, the Krüger series method converges to the exact Gauss–Krüger projection and the truncated series are a useful basis for numerical approximations to the mapping.

There is no problem with the convergence of expression for A , Eq. (14). This can be written in closed form as

$$A = \frac{2a}{\pi} E(e) = \frac{2a}{\pi} E(4n/(1+n)^2),$$

where $E(k)$ is the complete elliptic integral of the second kind with modulus k (DLMF, Eq. (19.2.8)), which may be expanded in a series using DLMF, Eq. (19.5.2) to give

$$A = \frac{a}{1+n} \left(1 + \frac{1}{4}n^2 + \frac{1}{64}n^4 + \frac{1}{256}n^6 + \frac{25}{16384}n^8 + \dots\right). \quad (29)$$

This series converges for $|n| < 1$ and, for small n , the relative error in truncating the series is given by the first dropped term.

The convergence of Eqs. (5) and (6) is more complicated because the sine terms in the summands become large for large η or η' . Indeed, the transverse Mercator projection has a singularity in its second derivative at $\phi = 0^\circ$ and $\lambda = \pm\lambda_0$ where $\lambda_0 = (1 - e)90^\circ$ beyond which the series will diverge; these points are branch points of the mapping (Whittaker and Watson, 1927, §5.7) and the properties of the mapping in their vicinity are explored in Sect. 5. In order to determine the error in the truncated series, I implement the formulas for the *exact* mapping as given by Lee (1976, §§54–55) who credits E. H. Thompson (1945) for their development. A referee has pointed out to me that a similar formulation was independently provided by Ludwig (1943). Here I give only a brief description of Lee’s method, referring the reader to the documentation and source code for GeographicLib for more details (Karney, 2010).

The exact mapping is expressed in terms of an intermediate mapping, the Thompson projection, denoted by $w = u + iv$ with (Lee, 1976, Eqs. (54.5) and (55.5))

$$\chi = \tanh^{-1} \operatorname{sn} w - e \tanh^{-1}(e \operatorname{sn} w), \quad (30)$$

$$\zeta = \frac{\pi}{2E(e)}(E(e) - \mathcal{E}(K(e) - w, e)), \quad (31)$$

where $\operatorname{sn} u$ is one of the Jacobi elliptic functions with modulus e (DLMF, §22.2), $K(k)$ is the complete elliptic integral of the first kind with modulus k (DLMF, Eq. (19.2.8)), and $\mathcal{E}(x, k)$ is Jacobi’s epsilon function (DLMF, Eq. (22.16.20)).

When implementing these equations, I follow Lee and break the formulas in terms of their real and imaginary parts. This enables the algorithm to be implemented with real arithmetic which allows the expressions to be optimized to minimize the round-off error. The necessary formulas for Eqs. (30) and (31) are given by Lee (1976, Eqs. (54.17) and (55.4)).

The computation of the forward (resp. reverse) mapping requires the inversion of Eq. (30) (resp. Eq. (31)). I perform these inversions using Newton’s method in the complex plane. The needed derivative of χ is given by Lee (1976, Eq. (54.21)) and $d\zeta/dw$ is given by Lee (1976, Eq. (55.9)) which may be split into real and imaginary parts with DLMF, Eq. (22.8.3), §22.6(iv). The starting guesses for Newton’s method are obtained by finding approximate solutions using one of three methods: (a) by using the limit $e \rightarrow 0$, (b) by expanding about the branch point on the equator (the bottom right corner of Fig. 3(c)), or (c) by expanding about the singularity at the south pole (the top right corner of Fig. 3(c)). (The latter two methods require a knowledge of the properties of the mapping far from the central meridian; see Sect. 5 for more information.) The most time-consuming task in this implementation was optimizing the choice of starting point to ensure that the method converges in a few iterations. I refer the reader to the code for details. I also compute the meridian convergence and scale using Lee (1976, Eqs. (55.12–13)).

In order to reduce the round-off errors, I needed to identify terms in the formulas with the potential for a loss of precision and apply identities for the Jacobi elliptic functions (DLMF, Eq. (22.2.10), §22.6(i)) to recast the formulas into equivalent ones with better numerical properties. I use the procedure *sncndn* given by Bulirsch (1965) for the elliptic functions and

algorithms R_F , R_D , and R_G of Carlson (1995) for the elliptic integrals; these algorithms can yield results to arbitrary precision.

I provide two implementations of the exact mapping: (a) a C++ version using standard floating-point arithmetic and (b) an implementation in Maxima (2009). The latter implementation makes use of Maxima’s “bigfloat” package which permits the calculation to be carried out to an arbitrary precision. This was used to construct a large test set for the mapping which served to benchmark the C++ implementation. This set includes randomly distributed points together with additional points chosen close to the pole and other possibly problematic points and lines. The mapping is computed to an accuracy of 80 decimal digits and the results are rounded to the nearest 0.1 pm. Both the C++ and Maxima implementations of the exact mapping and the test data are provided with GeographicLib (Karney, 2010).

The C++ implementation was checked by computing the maximum of the error in the forward mapping expressed as a true distance (i.e., dividing the error in the mapped space by the scale of the mapping) and the error in the reverse mapping (again expressed as a true distance). When implemented using double (resp. extended) precision, the maximum round-off error is $\delta_r = 9$ nm (resp. 5 pm) over the whole ellipsoid (using the WGS84 parameters, $a = 6\,378\,137$ m and $f = 1/298.257\,223\,563$). These are consistent with $\delta_r \approx M/2^{p-3}$ indicating that the error is only about 8 times the limiting round-off error given in Sect. 1. The truncation error δ_t , defined in Sect. 4, is zero for this method.

Using the double precision implementation, the errors in the meridian convergence and scale at a particular point are bounded by

$$\delta\gamma_r < \frac{1}{2^{p-3}} \left(1 + \frac{M}{s_p} + 1.5 \sqrt[3]{\frac{M}{s_b}} \right) \frac{180^\circ}{\pi},$$

$$\frac{\delta k_r}{k} < \frac{1}{2^{p-3}} \left(1 + 1.5 \sqrt[3]{\frac{M}{s_b}} \right),$$

where s_p and s_b are the geodesic distances from the point to the closest pole and closest branch point, respectively. These bounds were found empirically; however the form of the expressions is determined by the nature of the singularities in the mapping. The term involving s_p arises because small errors in the position close to the pole may cause large changes in the convergence. Similarly the terms involving s_b appear because of the singularity in the second derivative of the mapping which causes the convergence and scale to vary rapidly near the branch point.

The differences between my implementation and that of Dozier (1980) are as follows. (a) Dozier’s starting guesses for Newton’s method are based only on the limit $e \rightarrow 0$. Newton’s method then fails to converge in the neighborhood of the branch point (where ellipsoidal effects become large). In contrast, I use different methods for computing the starting points in different regions which enables Newton’s method to converge everywhere. (b) I modified several of the equations to improve the numerical accuracy. Without this, Dozier loses about half the precision in some regions. (c) I use published

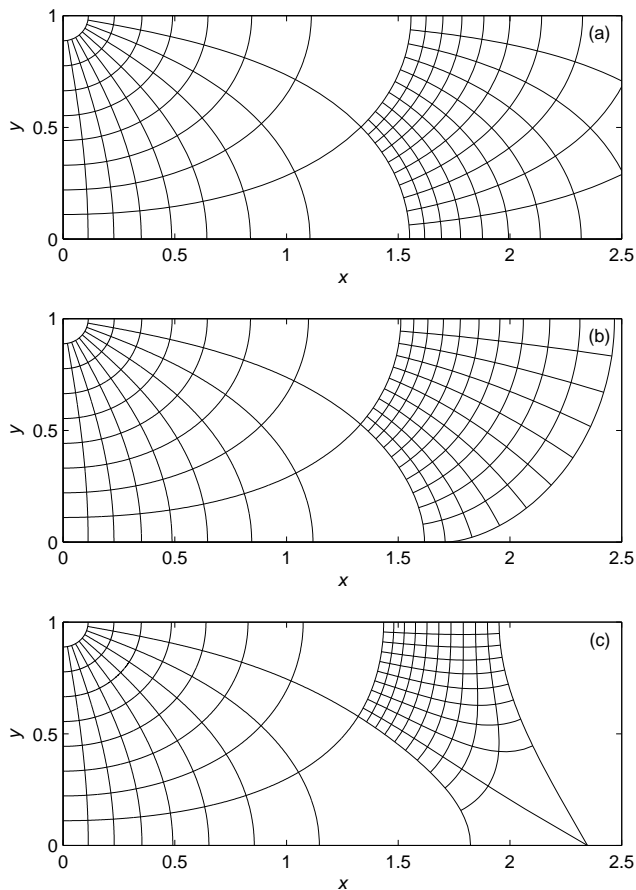


FIG. 1 Graticules for the (a) spherical transverse Mercator, (b) Gauss–Krüger, and (c) Thompson projections. Here x and y are the easting and northing for the mappings. The eccentricity is $e = \frac{1}{10}$ ($f \approx 1/199.5$) and the mappings have been scaled so that the distance from the equator to the north pole is unity. Thus $\lambda = 0^\circ$ maps to the line $x = 0$ and $\lambda = 90^\circ$ maps to the line $y = 1$. The graticule is shown at multiples of 10° with 1° lines added in $80^\circ < \lambda < 90^\circ$ and $0 < \phi < 10^\circ$.

algorithms to evaluate the special functions (Bulirsch, 1965; Carlson, 1995). (d) I compute the meridian convergence and scale. (e) Lastly, I provide an arbitrary precision implementation (in Maxima) to allow the errors in the C++ implementation to be measured accurately.

Figures 1(b) and (c) show the graticule for the Gauss–Krüger and Thompson projections. One eighth of the ellipsoid is shown in these figures, $0^\circ \leq \phi \leq 90^\circ$ and $0^\circ \leq \lambda \leq 90^\circ$, and (unlike the spherical transverse Mercator projection, Fig. 1(a) this maps to a finite area with the Gauss–Krüger and Thompson projections. To obtain the graticule for the entire ellipsoid, reflect these figures in $x = 0$, $y = 0$, and $y = 1$. The eccentricity for these figures is $e = \frac{1}{10}$ and, in this case, the equator runs along $y = 0$ until the branch point at $\lambda = \lambda_0 = 81^\circ$ and then heads for $y = 1$; the point $\phi = 0^\circ$, $\lambda = 90^\circ$ maps to finite points on $y = 1$. The Thompson mapping is not conformal at the branch point (where there’s a kink in the equator), because $d\chi/dw$ vanishes there. Similar

figures are given by Lee (1976, Figs. 43–46).

4. EXTENDING KRÜGER’S SERIES

There are several ways that the series for A , α_j and β_j can be generated; here, I adopt an approach which is close to that used by Krüger (1912, §5). (Alternative methods are to expand Eqs. (30) and (31) or to use the polar stereographic projection instead of the Mercator projection as the starting point (Wallis, 1992).) In the limit $\eta = \eta' = 0$ (i.e., on the central meridian, $\lambda = 0$), the quantities ζ and ζ' become the rectifying and conformal latitudes respectively. (The conformal latitude ϕ' was introduced in Sect. 2; the rectifying latitude is linearly proportional to the distance along a meridian measured from the equator.) The transformation between ζ and ζ' is thus given by the relation between the rectifying and conformal latitudes extended to the complex plane. Thus ζ is the meridian distance scaled to $\pi/2$,

$$\zeta(\Phi) = \frac{\pi}{2E(e)} \int_0^\Phi \frac{1 - e^2}{(1 - e^2 \sin^2 \phi)^{3/2}} d\phi, \quad (32)$$

where Φ is the normal geographic latitude extended to the complex plane. The integral here can be expressed in terms of elliptic integrals as $E(e) - E(\Theta, e)$, where $E(\phi, k)$ is the incomplete elliptic integral of the second kind with argument ϕ and modulus k (DLMF, Eq. (19.2.5)), and $\Theta = \cot^{-1}((1 - f) \tan \Phi)$ is the parametric co-latitude. Similarly, ζ' is merely Eq. (4) extended to the complex plane.

$$\zeta'(\Phi) = \text{gd}(\text{gd}^{-1} \Phi - e \tanh^{-1}(e \sin \Phi)). \quad (33)$$

The quantities Φ and Θ are related to the Thompson projection variable w by

$$\begin{aligned} \Phi &= \text{am } w, & \Theta &= \text{am}(K(e) - w), \\ w &= F(\Phi, e) = K(e) - F(\Theta, e), \end{aligned} \quad (34)$$

where $\text{am } w$ is Jacobi’s amplitude function (DLMF, §22.16(i)) with modulus e and $F(\phi, k)$ is the incomplete elliptic integral of the first kind with argument ϕ and modulus k (DLMF, Eq. (19.2.4)). Substituting Eq. (34) into Eqs. (33) and (32) and using Eq. (2) and DLMF, Eq. (22.16.31) gives Eqs. (30) and (31); this establishes the equivalence of Eqs. (32) and (33) with the formulation of Lee (1976). These equations are used by Stuifbergen (2009) as the basis for an exact numerical method for the transverse Mercator projection. This is similar to (but rather simpler than) the method of Dozier (1980).

The functions $\zeta(\Phi)$ and $\zeta'(\Phi)$ are analytic and so define conformal transformations. They can be expanded as a Taylor series in e^2 , or equivalently in n ; I use the method of Lagrange (1770, §16) (Whittaker and Watson, 1927, §7.32) to invert these series to give the inverse functions $\Phi(\zeta)$ and $\Phi(\zeta')$. For example, if

$$\zeta(\Phi) = \Phi + g(\Phi),$$

where $g(\Phi) = O(n)$, then the inverse function is

$$\Phi(\zeta) = \zeta + h(\zeta),$$

where

$$h(\zeta) = \sum_{j=1}^{\infty} \frac{(-1)^j}{j!} \left. \frac{d^{j-1}g(\Phi)^j}{d\Phi^{j-1}} \right|_{\Phi=\zeta}.$$

Now compose $\zeta(\Phi(\zeta'))$ and $\zeta'(\Phi(\zeta))$ to provide the required series, Eqs. (5) and (6). These manipulations were carried out using the algebraic tools provided by Maxima (2009). Little effort was expended to optimize this calculation since it only needs to be carried out once! (The expansion to order n^8 takes about 15 seconds.) At 8th order, the series for A is given by Eq. (29) and the series for α_j , Eq. (12), and β_j , Eq. (17), become

$$\begin{aligned} \alpha_1 &= \frac{1}{2}n - \frac{2}{3}n^2 + \frac{5}{16}n^3 + \frac{41}{180}n^4 - \frac{127}{288}n^5 + \frac{7891}{37800}n^6 \\ &\quad + \frac{72161}{387072}n^7 - \frac{18975107}{50803200}n^8 + \dots, \\ \alpha_2 &= \frac{13}{48}n^2 - \frac{3}{5}n^3 + \frac{557}{1440}n^4 + \frac{281}{630}n^5 - \frac{1983433}{1935360}n^6 \\ &\quad + \frac{13769}{28800}n^7 + \frac{148003883}{174182400}n^8 + \dots, \\ \alpha_3 &= \frac{61}{240}n^3 - \frac{103}{140}n^4 + \frac{15061}{26880}n^5 + \frac{167603}{181440}n^6 - \frac{67102379}{29030400}n^7 \\ &\quad + \frac{79682431}{79833600}n^8 + \dots, \\ \alpha_4 &= \frac{49561}{161280}n^4 - \frac{179}{168}n^5 + \frac{6601661}{7257600}n^6 + \frac{97445}{49896}n^7 \\ &\quad - \frac{40176129013}{7664025600}n^8 + \dots, \\ \alpha_5 &= \frac{34729}{80640}n^5 - \frac{3418889}{1995840}n^6 + \frac{14644087}{9123840}n^7 \\ &\quad + \frac{2605413599}{622702080}n^8 + \dots, \\ \alpha_6 &= \frac{212378941}{319334400}n^6 - \frac{30705481}{10378368}n^7 + \frac{175214326799}{58118860800}n^8 + \dots, \\ \alpha_7 &= \frac{1522256789}{1383782400}n^7 - \frac{16759934899}{3113510400}n^8 + \dots, \\ \alpha_8 &= \frac{1424729850961}{743921418240}n^8 + \dots, \end{aligned} \quad (35)$$

and

$$\begin{aligned} \beta_1 &= \frac{1}{2}n - \frac{2}{3}n^2 + \frac{37}{96}n^3 - \frac{1}{360}n^4 - \frac{81}{512}n^5 + \frac{96199}{604800}n^6 \\ &\quad - \frac{5406467}{38707200}n^7 + \frac{7944359}{67737600}n^8 + \dots, \\ \beta_2 &= \frac{1}{48}n^2 + \frac{1}{15}n^3 - \frac{437}{1440}n^4 + \frac{46}{105}n^5 - \frac{1118711}{3870720}n^6 \\ &\quad + \frac{51841}{1209600}n^7 + \frac{24749483}{348364800}n^8 + \dots, \\ \beta_3 &= \frac{17}{480}n^3 - \frac{37}{840}n^4 - \frac{209}{4480}n^5 + \frac{5569}{90720}n^6 + \frac{9261899}{58060800}n^7 \\ &\quad - \frac{6457463}{17740800}n^8 + \dots, \\ \beta_4 &= \frac{4397}{161280}n^4 - \frac{11}{504}n^5 - \frac{830251}{7257600}n^6 + \frac{466511}{2494800}n^7 \\ &\quad + \frac{324154477}{7664025600}n^8 + \dots, \\ \beta_5 &= \frac{4583}{161280}n^5 - \frac{108847}{3991680}n^6 - \frac{8005831}{63866880}n^7 \\ &\quad + \frac{22894433}{124540416}n^8 + \dots, \\ \beta_6 &= \frac{20648693}{638668800}n^6 - \frac{16363163}{518918400}n^7 \\ &\quad - \frac{2204645983}{12915302400}n^8 + \dots, \\ \beta_7 &= \frac{219941297}{5535129600}n^7 - \frac{497323811}{12454041600}n^8 + \dots, \\ \beta_8 &= \frac{191773887257}{3719607091200}n^8 + \dots. \end{aligned} \quad (36)$$

GeographicLib (Karney, 2010) includes the Maxima code for carrying out these expansions and the results of expanding the series much further, to order n^{30} .

Equations (29), (35), and (36) allow the Krüger method to be implemented to any order up to n^8 . In order to determine

which order to use in a given application, it is useful to distinguish the truncation error (the difference between the series evaluated exactly and the exact mapping) from the round-off error (the difference between the series evaluated at finite precision and the series evaluated exactly).

The truncation error was determined using Maxima's big-floats with a precision of 80 decimal digits. With Krüger's series the error is principally a function of distance from the meridian (which is mainly a function of x) and depends only weakly on y . Defining s_m as the geodesic distance from the central meridian, I measure δ_t the maximum of the forward and reverse truncation errors (both expressed as true distances) over all points with a given s_m . In Fig. 2, I plot δ_t as a function of s_m , for truncations at various orders J (the smallest terms retained are n^J). The errors rise monotonically with the distance from the central meridian. The branch point at $\phi = 0^\circ$ and $\lambda = \lambda_0 \approx 82.636^\circ$ is at about $s_m = 9200$ km. At this point the truncation error stops decreasing with increasing order indicating a lack of convergence in the series. (See Sect. 5 for a proof.) From a practical standpoint, the convergence is too slow to be useful for $s_m \gtrsim 8000$ km. The truncation errors in the meridian convergence $\delta\gamma_t$ and scale δk_t are well approximately by

$$\begin{aligned} \delta\gamma_t &= 2J \sec(s_m/a) \frac{\delta_t}{a} \frac{180^\circ}{\pi}, \\ \frac{\delta k_t}{k} &= 2J \sec(s_m/a) \frac{\delta_t}{a}. \end{aligned}$$

Here, the factor $2J$ arises from the differentiation performed to give Eqs. (23) and (26) and the term $\sec(s_m/a)$ is the scale (in the spherical limit) necessary to convert the errors in position to errors in ζ or ζ' .

Figure 2 epitomizes the advantages of Krüger's over Thomas' series. The equivalent figure for truncation error for the latter series would use the *longitude* relative to the central meridian instead of the *distance* from the central meridian. At high latitudes, the longitude difference becomes large even for modest distances from the central meridian; this explains the large errors in the results from Geotrans in the Greenland example at the end of Sect. 2.

Round-off errors need to be considered also when implementing the method with floating-point arithmetic. Evaluating the mapping using the formulas given in Sect. 2 adds 4.2 nm or 1.9 pm to the truncation error depending on the precision (see the dashed lines in Fig. 2). These round-off errors may be expressed as $\delta_r \approx M/2^{p-2}$; i.e., they are about half of those for the exact algorithm, because the series method involves fewer operations. Thus with double (resp. extended) precision and the series truncated at $J = 6$ (resp. $J = 8$) the overall error is less than 5 nm (resp. 2 pm) provided that $s_m < 3900$ km (resp. 4200 km). The C++ implementation of the mapping based on the extended Krüger series (taken to order n^8) is included in GeographicLib (Karney, 2010).

At greater distances from the central meridian, truncation errors become large; thus the 6th order series has an error of about 1 mm at $s_m = 7600$ km (see Fig. 2). The truncation error can be decreased by increasing the number of terms retained in the series. However, if high accuracy is required for

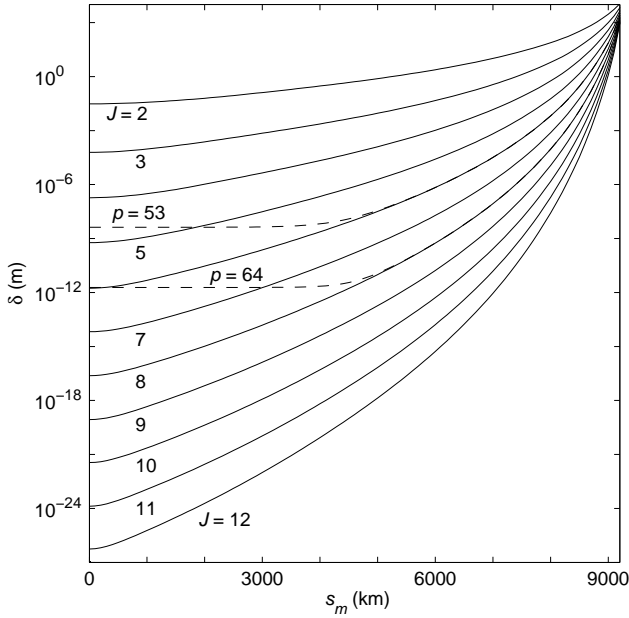


FIG. 2 Truncation and round-off errors, δ_t and δ_r , in the Krüger series for the transverse Mercator projection as a function of the distance from the central meridian s_m . The series is truncated at various orders J from 2 to 12. The solid lines show the δ_t . Also shown in dashed lines are the combined round-off and truncation errors, $\delta_t + \delta_r$ when the algorithm is implemented with floating-point numbers with p bits of fraction. For $p = 53$ (double) and $p = 64$ (extended), the truncation levels are set to $J = 6$ and $J = 8$ respectively. The WGS84 ellipsoid is used.

$s_m \gtrsim 4000$ km, it's probably safer to use the exact algorithm whose error is less than 9 nm for the whole spheroid.

The round-off errors in the meridian convergence and scale are bounded by

$$\delta\gamma_r < \frac{1}{2^{p-3}} \left(1 + 0.5 \frac{M}{s_p}\right) \frac{180^\circ}{\pi}, \quad \frac{\delta k_r}{k} < \frac{1}{2^{p-3}};$$

these should be added to $\delta\gamma_t$ and δk_t . These expressions have the same form as those for the exact algorithm, except that the terms involving s_b are omitted because the truncation error dominates near the branch point.

Previously, Engsager and Poder (2007) extended Krüger's series to 7th order. However they give a less rigorous estimate of the error. In addition, they give separate series for the meridian convergence and scale, while I advocate following Krüger's simpler prescription of differentiating the same series used to carry out the mapping. They also give a series expansion for the transformation between latitude and conformal latitude which leads to a somewhat faster code (see Sect. 6); however, I prefer the simplicity of evaluating and inverting Eq. (7) directly.

5. PROPERTIES FAR FROM THE CENTRAL MERIDIAN

In this section, I explore the behavior of the mapping in the vicinity of the branch point at $\phi = 0^\circ$ and $\lambda = \lambda_0$. First it should be remarked that this is far from the central meridian and that the scale there is k_0/e ; so this is not in the domain where the mapping is very useful. Nevertheless, it is beneficial to have a complete understanding of a mapping; for example, this was necessary in making the exact algorithm robust. Here I describe the mapping in terms of the Thompson mapping, w (Lee, 1976, §§54–55). König and Weise (1951) offer a complementary picture based on the complex latitude Φ .

The transverse Mercator projection is defined by its properties on the central meridian and the condition of conformality. The mapping is defined by analytically continuing (Whittaker and Watson, 1927, Chap. 5) the mapping away from the central meridian. The process continues until the branch point is encountered (where the condition of analyticity fails). The branch point corresponds to $\chi = \chi_0 = i\lambda_0$, $\zeta = \zeta_0 = i(K' - E')\pi/(2E)$, and $w = w_0 = iK'$, where $E = E(e)$, $E' = E(\sqrt{1-e^2})$, $K = K(e)$, $K' = K(\sqrt{1-e^2})$, and $K(k)$ is the complete elliptic integral of the first kind with modulus k (DLMF, Eq. (19.2.8)). The lowest order terms in the expansions of χ and ζ about the branch point are

$$\begin{aligned} \tilde{\chi} &= -\frac{1}{3}e(1-e^2)\left[\tilde{w}^3 + \frac{1}{10}(1+e^2)\tilde{w}^5 + \dots\right], \\ \tilde{\zeta} &= -\frac{1}{3}(1-e^2)\left[\tilde{w}^3 + \frac{1}{5}(2-e^2)\tilde{w}^5 + \dots\right]\pi/(2E), \end{aligned}$$

where $\tilde{\chi} = \chi - \chi_0$, $\tilde{\zeta} = \zeta - \zeta_0$, and $\tilde{w} = w - w_0$. Eliminating w from these equations gives

$$\tilde{\zeta} = \frac{\pi}{2E} \left[\frac{\tilde{\chi}}{e} + \frac{i\sqrt{1-e^2}}{10} \left(\frac{3i\tilde{\chi}}{e} \right)^{5/3} + O(\tilde{\chi}^{7/3}) \right]. \quad (37)$$

The value of ζ will depend on how the $\frac{5}{3}$ power is taken. Picking the complex phase of $i\tilde{\chi}$ in the interval $(-\pi, \pi]$ gives the principal value. Equivalently, the value of $\zeta(\chi)$ can be made single valued by placing “cuts” on the equator in the longitude ranges $(1-e)90^\circ \leq |\lambda| \leq (1+e)90^\circ$ which act as impassable barriers during the process of analytic continuation. This represents the “standard” convention for mapping a geographic position to the Gauss–Krüger projection since the sign of the northing matches the sign of the latitude (with the equator mapping to non-negative northings). This convention corresponds to Fig. 1(b) (after suitable reflections to cover the ellipsoid), to Lee (1976, Fig. 46), to König and Weise (1951, Fig. 55(b)), and to Ludwig (1943, p. 214).

From the form of the mapping near the branch point, it is clear that the Krüger series does not converge for $\phi = 0$ and $\lambda > \lambda_0$ because, from Eq. (37), ζ is complex under these conditions but all the terms in the series, Eq. (5), are pure imaginary. Delineating the precise boundary for convergence of the series and its inverse, Eq. (6), requires an analysis of the problem for complex e and is beyond the scope of this work.

It is possible to extend the mapping by moving to the “right” of the equator in Fig. 1(b). If the complex phase of $i\tilde{\chi}$ includes the interval $[0, \frac{3}{2}\pi]$, an “extended” domain for the mapping may be defined by the union of $0^\circ \leq \phi \leq 90^\circ$,

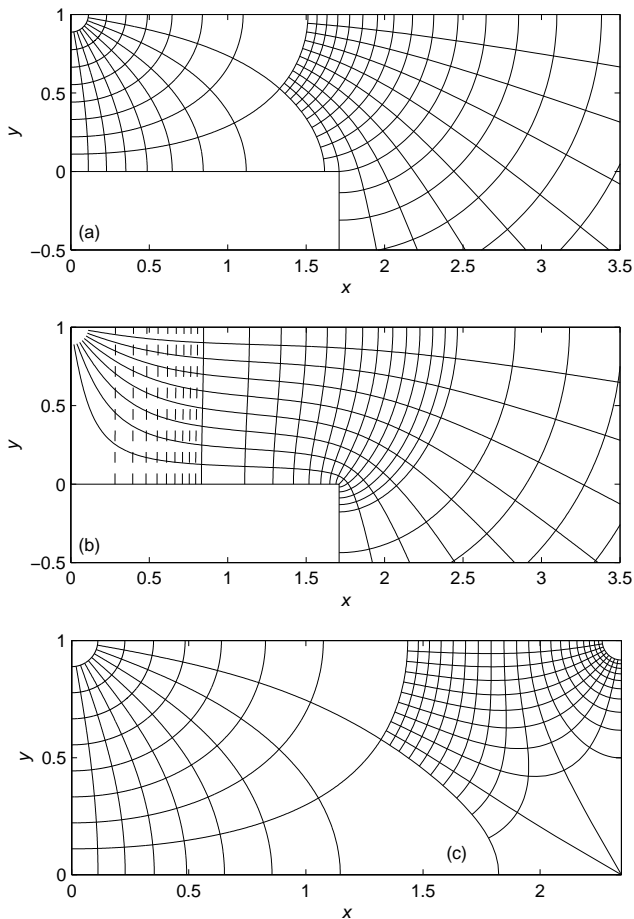


FIG. 3 Extended transverse Mercator projection. (a) shows the graticule and (b) the convergence and scale for Gauss–Krüger projection. (c) shows the graticule for the Thompson projection. The ellipsoid parameters are the same as for Fig. 1. The graticules in (a) and (c) are the same as in Fig. 1(b) with the addition of 1° lines for $80^\circ < \lambda < 90^\circ$ and $-10^\circ \leq \phi < 0^\circ$. In (b), the lines emanating from the top left corner are lines of constant meridian convergence, γ , at 10° intervals. The dog-legged line joining $(0, 1)$, $(0, 0)$, $(1.71, 0)$, and $(1.71, -\infty)$ represents $\gamma = 0^\circ$. The line $y = 1$ gives $\gamma = 90^\circ$. The other lines (running primarily vertically in the figure) are lines of constant scale k . The solid lines show integer values of k for $1 \leq k \leq 15$ and multiples of 5 for $15 \leq k \leq 35$. The line segment joining $(0, 0)$ and $(0, 1)$ gives $k = 1$. The dashed lines show lines of constant k at intervals of 0.1 for $1 < k < 2$.

$0^\circ \leq \lambda \leq 90^\circ$ and $-90^\circ < \phi \leq 0^\circ$, $\lambda_0 \leq \lambda \leq 90^\circ$. The rule for analytic continuation is that the second region is reached by a path from the central meridian which goes north of the branch point. This is equivalent to placing the cut so that it emanates from the branch point in a south-westerly direction. Following this prescription, the range of the mapping now consists of the union of $0 \leq x$, $0 \leq y/(k_0a) \leq E$ and $K' - E' \leq x/(k_0a)$, $y \leq 0$.

Figures 3(a) and (b) illustrate the properties of the Gauss–Krüger projection in this extended domain. These figures use an ellipsoid with eccentricity $e = \frac{1}{10}$ (as in Fig. 1) and with $a = 1/E = 0.6382$ and $k_0 = 1$. The branch point then lies

at $\phi = 0^\circ$, $\lambda = 81^\circ$ or $x = (K' - E')/E \approx 1.71$, $y = 0$. Symmetries can now be employed to extend the mapping with arbitrary rules for how to circumvent the branch point. The symmetries are equivalent to placing mirrors on the four lines segments: $0 \leq x$, $y = 1$; $x = 0$, $0 \leq y \leq 1$; $0 \leq x \leq 1.71$, $y = 0$; and $x = 1.71$, $y \leq 0$. Compare Fig. 3(a) with König and Weise (1951, Fig. 53(b)).

Figure 3(c) shows the graticule of the Thompson projection in the extended domain; the range of this mapping is the rectangular region shown, $0 \leq x/(k_0a) \leq K'$, $0 \leq y/(k_0a) \leq K$. The extended Thompson projection has reflection symmetry on all the four sides of Fig. 3(c). In transforming from Thompson to Gauss–Krüger, the right angle at the lower right corner of Fig. 3(c) expands by a factor of 3 to 270° to produce the outside corner at $x = 1.71$, $y = 0$ in Fig. 3(a). The top right corner of Fig. 3(c) represents the south pole and this is transformed to infinity in the extended Gauss–Krüger projection. Despite the apparent similarities, the behavior of the extended Thompson projection near the north and south poles (the top left and top right corners in Fig. 3(c)) is rather different. Although the mapping at north pole is conformal, the mapping at the south pole in the extended domain is not. The difference in longitude between the two meridians represent by the top and right edges of Fig. 3(c) is $90^\circ e$ instead of 90° .

My implementation of the exact mapping provides the option of using the extended domain. The round-off errors quoted in Sect. 3 (9 nm for double precision and 5 μ m for extended precision) apply to the extended domain for $\phi > -15^\circ$. Beyond this line, the errors grow because of the contraction of w space near the south pole (at $\phi = -58^\circ$, the error is about 1 mm).

6. CONCLUSION

The algorithms presented here allow the transverse Mercator projection to be computed with an accuracy of a few nanometers. Implementations of these algorithms are included in GeographicLib (Karney, 2010) which also provides (a) the set of test data used to check the implementations, (b) Maxima code for the exact mapping (with arbitrary precision), (c) Maxima code for generating the Krüger series to arbitrary order, and (d) the Krüger series to 30th order. The web page <http://geographiclib.sf.net/tm.html> provides quick links to all these resources.

The work described in this paper made heavy use of the computer algebra system Maxima (2009) both for carrying out the series expansions for Krüger’s method and for generating the high accuracy test data. The latter is invaluable when developing complex algorithms with an accuracy close to machine precision. Other computer algebra systems offer similar capabilities; but Maxima is one of the few that is free.

My emphasis in developing these algorithms was in their accuracy. Nevertheless the resulting implementations are reasonably fast. On a 2.66 GHz Intel processor and compiled with g++, the time for the mappings implemented with the 6th order series method is 1.91 μ s; this is the combined time for a forward and a reverse mapping including the computation of

the convergence and scale in each case. This time is insensitive to number of terms retained in the sum due to the efficiency of Clenshaw summation—changing this to 4 (resp. 8) decreases (resp. increases) the time by only 1%. Skipping the calculation of the convergence and scale reduces the time by 15%. Using a trigonometric series and Clenshaw summation for the conversions between geographic and conformal latitude (as proposed by Engsager and Poder (2007)) decreases the time by 18%. The exact algorithms (which are accurate over the entire ellipsoid) are 5–6 times slower. The 6th order series method is comparable in speed to Geotrans 3.0 even though the latter is much less accurate and does not return the convergence and scale.

Here are some recommendations for users of the transverse Mercator projection. Do not use algorithms based on the formulas given by Thomas (1952)—they are unnecessarily inaccurate. Instead use the Krüger series, truncating Eqs. (29), (35), and (36) to order n^6 . With double precision, this gives an accuracy of 5 nm for distances up to 3900 km from the central meridian. If the mapping is needed at greater distances from the central meridian, use the algorithm based on the exact mapping (an accuracy of 9 nm). If greater accuracy is needed, use extended precision with either method (extending the series method to 8th order). When implementing these algorithms, use the test set to verify that the errors are comparable with those given here.

Acknowledgments

I would like to thank Rod Deakin and Knud Poder for helpful discussions.

References

- L. M. Bugayevskiy and J. P. Snyder, 1995, *Map Projections: A Reference Manual* (Taylor & Francis, London), <http://www.worldcat.org/oclc/31737484>.
- R. Bulirsch, 1965, *Numerical calculation of elliptic integrals and elliptic functions*, *Num. Math.*, **7**(1), 78–90, doi: 10.1007/BF01397975.
- B. C. Carlson, 1995, *Numerical computation of real or complex elliptic integrals*, *Numerical Algorithms*, **10**(1), 13–26, doi: 10.1007/BF02198293, E-print arXiv:math/9409227.
- C. W. Clenshaw, 1955, *A note on the summation of Chebyshev series*, *Math. Tables Aids Comput.*, **9**(51), 118–120, <http://www.jstor.org/stable/2002068>.
- J. Dozier, 1980, *Improved algorithm for calculation of UTM and geodetic coordinates*, Technical Report NESS 81, NOAA, <http://fiesta.bren.ucsb.edu/~dozier/Pubs/DozierUTM1980.pdf>.
- K. E. Engsager and K. Poder, 2007, *A highly accurate world wide algorithm for the transverse Mercator mapping (almost)*, in *Proc. XXIII Intl. Cartographic Conf. (ICC2007), Moscow*, p. 2.1.2.
- Geotrans, 2010, *Geographic translator, version 3.0*, <http://earth-info.nga.mil/GandG/geotrans/>.
- J. W. Hager, J. F. Behensky, and B. W. Drew, 1989, *The universal grids: Universal Transverse Mercator (UTM) and Universal Polar Stereographic (UPS)*, Technical Report TM 8358.2, Defense Mapping Agency, <http://earth-info.nga.mil/GandG/publications/tm8358.2/TM8358.2.pdf>.
- C. F. F. Karney, 2010, *GeographicLib, version 1.7*, <http://geographiclib.sf.net>.
- R. König and K. H. Weise, 1951, *Mathematische Grundlagen der Höheren Geodäsie und Kartographie*, volume 1 (Springer, Berlin).
- J. H. L. Krüger, 1912, *Konforme Abbildung des Erdellipsoids in der Ebene*, New Series 52, Royal Prussian Geodetic Institute, Potsdam, doi:10.2312/GFZ.b103-krueger28.
- R. Kuittinen, T. Sarjakoski, M. Ollikainen, M. Poutanen, R. Nuuros, P. Tätilä, J. Peltola, R. Ruotsalainen, and M. Ollikainen, 2006, *ETRS89—järjestelmään liittyvät karttaprojektiot, tasokoordinaattistot ja karttalehtijako*, Technical Report JHS 154, Finnish Geodetic Institute, Appendix 1, Projektiokaavart, http://docs.jhs-suositukset.fi/jhs-suositukset/JHS154/JHS154_liite1.pdf.
- J. L. Lagrange, 1770, *Nouvelle méthode pour résoudre les équations littérales par le moyen des séries*, in *Oeuvres*, volume 3, pp. 5–73 (Gauthier-Villars, Paris, 1869), reprint of *Mém. de l'Acad. Roy. des Sciences de Berlin* **24**, 251–326, <http://books.google.com/books?id=YywPAAAIAAJ&pg=PA5>.
- J. H. Lambert, 1772, *Anmerkungen und Zusätze zur Entwerfung der Land- und Himmelscharten*, number 54 in *Klassiker ex. Wiss.* (Engelmann, Leipzig, 1894), translated into English by W. R. Tobler as *Notes and Comments on the Composition of Terrestrial and Celestial Maps*, Univ. of Michigan (1972), http://books.google.com/books?id=o_s_MR3NUD4C.
- L. P. Lee, 1976, *Conformal projections based on Jacobian elliptic functions*, *Cartographica*, **13**(1, Monograph 16), 67–101, doi: 10.3138/X687-1574-4325-WM62.
- K. Ludwig, 1943, *Die der transversalen Mercatorkarte der Kugel entsprechende Abbildung des Rotationsellipsoids*, *J. Reine Angew. Math.*, **185**(4), 193–230, doi:10.1515/crll.1943.185.193, <http://resolver.sub.uni-goettingen.de/purl?GDZPPN002175576>.
- Maxima, 2009, *A computer algebra system, version 5.20.1*, <http://maxima.sf.net>.
- F. W. J. Olver, D. W. Lozier, R. F. Boisvert, and C. W. Clark, editors, 2010, *NIST Handbook of Mathematical Functions* (Cambridge Univ. Press), <http://dlmf.nist.gov>.
- N. Stuijbergen, 2009, *Wide zone transverse Mercator projection*, Technical Report 262, Canadian Hydrographic Service, <http://www.dfo-mpo.gc.ca/Library/337182.pdf>.
- P. D. Thomas, 1952, *Conformal projections in geodesy and cartography*, Special Publication 251, U.S. Coast and Geodetic Survey, http://docs.lib.noaa.gov/rescue/cgs_specpubs/QB275U35no2511952.pdf.
- D. E. Wallis, 1992, *Transverse Mercator projection via elliptic integrals*, Technical Report NPO-17996, JPL.
- E. T. Whittaker and G. N. Watson, 1927, *A Course of Modern Analysis* (Cambridge Univ. Press), 4th edition, reissued in Cambridge Math. Library Series (1996).